FATIGUE CRACK GROWTH BEHAVIOUR OF FRICTION STIR WELDED ALUMINIUM-LITHIUM ALLOY 2195 T8X

P.M.G.P Moreira[1], A.M.P. de Jesus[2], M.A.V. de Figueiredo[3], M. Windisch[4], G. Sinnema[5], P.M.S.T. de Castro[3]

[1] INEGI, Laboratório de Óptica e Mecânica Experimental - LOME, Porto, Portugal, pmoreira@inegi.up.pt
[2] Universidade de Trás-os-Montes e Alto Douro, Departamento de Engenharias, Vila Real, Portugal, ajesus@utad.pt
[3] Universidade do Porto, Faculdade de Engenharia, Departamento de Eng. Mecânica, Porto, Portugal, mfiguei@fe.up.pt
[4] MT Aerospace AG, Department TEA, Augsburg, Germany, michael.windisch@mt-aerospace.de
[5] European Space Agency ESA ESTEC, Noordwijk, the Netherlands, Gerben.Sinnema@esa.int

ABSTRACT

Al-Li alloys such as 2195 are candidate materials for reducing the structural weight of cryogenic tanks on launch vehicles due to their low density, high strength and fatigue crack growth resistance. Although there are many advantages with Al-Li alloys, important limitations remain while using conventional joining techniques. The present work was performed under the ESA TRP "Damage Tolerance of Cryogenic Pressure Vessels", a project aiming at defining potential applications for state of art Friction Stir Welding (FSW) techniques in cryogenic tanks for Expendable Launch Vehicle and Reusable Launch Vehicle.
The work presented in this paper involves the characterization of the fatigue performance of the AA2195-T8X at room temperature. SN fatigue tests and crack growth tests of base material and friction stir welded 5mm thick specimens of the AA2195-T8X were performed. For SN determination, tests were carried out at two different R ratios, 0.1 and 0.8, using for each stress ratio three different maximum loads. During crack growth tests, three different R ratios, 0.1, 0.5 and 0.8, were used per each three different material conditions - base material, heat affected zone (HAZ), and weld. Specimens containing notches at the centre of the weld, at the HAZ and at the base material, were tested. The first type of specimens has notches in the centre of the weld, which coincides with the centre of the weld nugget. In the second type of specimens the crack is located in the HAZ.

KEY WORDS: aluminium-lithium alloy, FSW, fatigue, fatigue crack growth tests.

1. INTRODUCTION

In the aeronautics and space industries one of the most effective ways to reduce weight is to reduce the density of the aluminum alloys used. For purposes of reducing the alloy density, lithium additions have been used. The rapid increase in solid solubility of lithium in aluminum over the temperature range of 0°C - 500°C results in an alloy system achieving, through precipitation hardening, good strength levels. However, the addition of Li to Al alloys presents problems, as possible decreases in ductility and fracture toughness, delamination problems and poor stress corrosion cracking resistance. Increased strength with only minimal or no decrease in toughness is therefore a major issue.

The interest in Al-Li alloys derives from the large effect that lithium additions have on the modulus of aluminum, a 6 percent increase for every weight percent added, and the density, a 3 percent decrease for every weight percent added, [1]. These changes apply for lithium additions up to 3 weight percent. There have been three early generations of Al-Li alloys, *(i)* those produced in the 50s to 70s, including alloys 2020 and 1420; these alloys experienced ductility and fracture toughness problems, or were of relatively low strength; *(ii)* those produced in the 1980s, including alloy 2090, 2091, 8090, and 8091, with high modulus and low density, but displaying anisotropic mechanical properties, and *(iii)* the more recent high-strength alloys as 2195. Al-Li alloys offer attractive properties for lightweight aerospace structures, due to their low density, high strength and fatigue crack growth resistance. Although there are many advantages with Al-Li alloys, important limitations remain while using conventional joining techniques. Friction Stir Welding (FSW) is a well established solid-state joining process that is expected to reduce many of the concerns about Al-Li welding. The present work was performed under the ESA TRP "Damage Tolerance of Cryogenic Pressure Vessels". The activity aims at defining potential applications for state of art FSW techniques in cryogenic tanks for Expendable Launch Vehicle and Reusable Launch Vehicle.

2. SN FATIGUE TESTS

INEGI performed SN fatigue tests at room temperature (RT) of friction stir welded (FSW) 5*mm* thick

specimens of the AA2195-T8X. Also, crack growth tests were carried out at room temperature for both base and welded materials. The test results of each specimen were linked to the specimen designation of the cut-off plan [2].
Preliminary tensile tests were performed at MT Aerospace in order to obtain the strength values of the AA2195-T8X friction stir welded material. These values, presented in Table 1, were used for the definition of the load levels of the fatigue tests and to determine the maximum load to be used on the fatigue sharpening and crack propagation procedures to prevent plasticity effects.

Table 1- Strength values for test definition and performance

	Temperature	$R_{p0.2}$ (σ_{yield})
2195 T8X	RT	510*MPa*
	77K (-196ºC)	650*MPa*
2195 T8X FSW	RT	300*MPa*
	77K (-196ºC)	380*MPa*

The stress life curves were evaluated according to [3, 4] using integral specimens perpendicular to the weld. The specimen geometry is presented in Figure 1 [5].

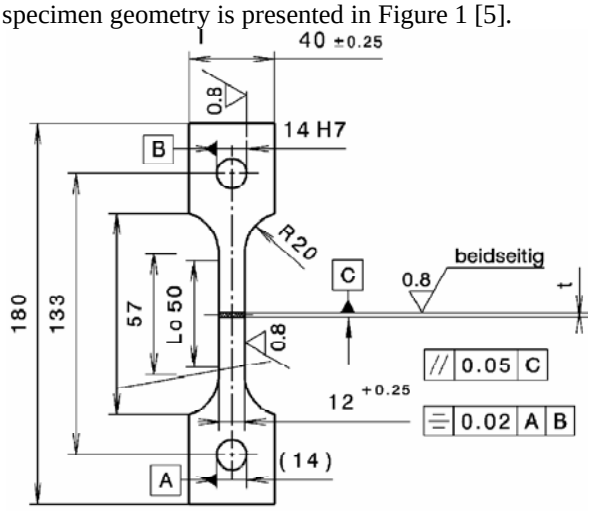

Figure 1- Geometry of the specimen to be use in the fatigue tests (SN).

For the calculation of the maximum loads to be applied in SN tests, the initial section is considered to be $5\times12=60mm^2$, and the FSW yield stress is the value presented in Table 1 (300*MPa*).
Tests were carried out at two different *R* ratios, 0.1 and 0.8, using for each stress ratio three different maximum loads. The *R* ratio of 0.1 represents pressure cycling (proof test, leak test etc.), and the R ratio of 0.8 represents external loads during operation. The tests were performed according to the matrix presented in Table 2.
These tests were carried out in a MTS 810 servo-hydraulic machine with a 100*kN* load cell.

Table 2- SN tests, definition of remote loads matrix

R ratio	Number of specimens	σ_{max}	Maximum load [*kN*]
0.1	2	FSW yield stress	18.00
	2	85% FSW yield stress	15.30
	2	70% FSW yield stress	12.60
0.8	1	FSW yield stress	18.00
	1	115% FSW yield stress	20.70
	1	130% FSW yield stress	23.40
	2	150% FSW yield stress	27.00

A mechanical grip fixture was developed in order to comply with the specimen geometry and maximum loads defined in the general test plan [5]. The geometry of each specimen was accurately measured before each test, especially in the section of the material affected by the welding process.

For the specimens tested at 70% of σ_{yield} some fatigue life scatter was found between the two tests; the first specimen fractured at around 800000 cycles and the second specimen remained un-fractured with a fatigue life of 10^7 cycles. Taking into account this observation a run out of 10^7 cycles was assumed. After this observation the option was to replace the third level of fatigue stress. Initially intended to be 50% of σ_{yield}, a value of 85% of σ_{yield} was chosen.
The first specimen tested with *R*=0.8, that corresponds to $\sigma_{max}=\sigma_{yield}$, did not fracture at 10^7 cycles. Taking into consideration this situation for *R*=0.8, instead of using the stress levels of 70% and 50% of yield stress previously defined, these two levels were replaced by 115% and 130% of σ_{yield}. Despite these changes in the test plan, all specimens tested at R=0.8 did not fracture at a fatigue life of 10^7 cycles. After this observation a higher level of remote stress, 150% of σ_{yield}, was used for the two remaining specimens. The plot of the fatigue lives for *R*=0.1 and *R*=0.8 is presented in Figure 2.

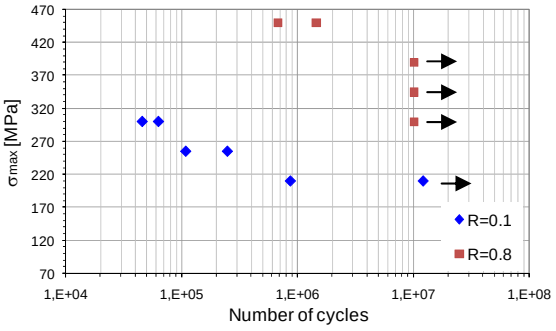

Figure 2- SN test results for *R*=0.1 and *R*=0.8.

When testing base material at R=0.1, max. stress corresponding to 10^5 cycles is of the order of 350 to 400 *MPa*, [6], whereas for the present FSW joints max. stress is of the order of 260 to 280 *MPa* for the same number of cycles, a reduction of just ~30%.
The location of the fracture surface in each SN specimen is presented in Table 3.

Table 3- Fracture surface identification in each SN specimen.

Spec	*R*	Advanc.or Retreat.	Crack initiat. surface	Weld zone
IT23	0.1	R	S	T
IT25	0.1	R	S	T
IT26	0.1	R	S	T
IT27	0.1		Did not break	
IT28	0.1	R	S	T
IT29	0.1	R	S	T
IT30	0.8		Did not break	
IT31	0.8		Did not break	
IT32	0.8		Did not break	
IT33	0.8	A	S	T
IT24	0.8	C	B	N

Table legend: A –Advancing; R- Retreading; C- Centre (weld line); S- Shoulder surface (crown surface); B- Bottom surface (root surface); T- Transition between material affected and material not affected by the shoulder (shoulder limit); N- Nugget.

Specimens IT23, IT25, IT26, IT28, IT29 and IT33 fractured in the transition from the stirred material to the base material, and the crack initiated near the surface where the shoulder contacted the plate. The IT24 specimen fractured at the centre of the weld.
The fracture initiation locations can be divided in three different groups, as presented in Table 4.

Table 4- Types of fracture location

Type	Specimens	Location
I	IT23; IT25; IT27; IT29;	Transition between material affected and material not affected by the shoulder (shoulder limit), and at the vertices of the specimen
II	IT26; IT28; IT33	Shoulder surface, at the centre of the weld line and at the middle of the specimen
III	IT24	Root surface, at the centre of the weld line and at the middle of the specimen

A macrograph of each type of fracture location found in the SN fatigue specimens is presented in Figure 3 (specs. IT23, IT26 and IT24, see a), b) and c) respectively).

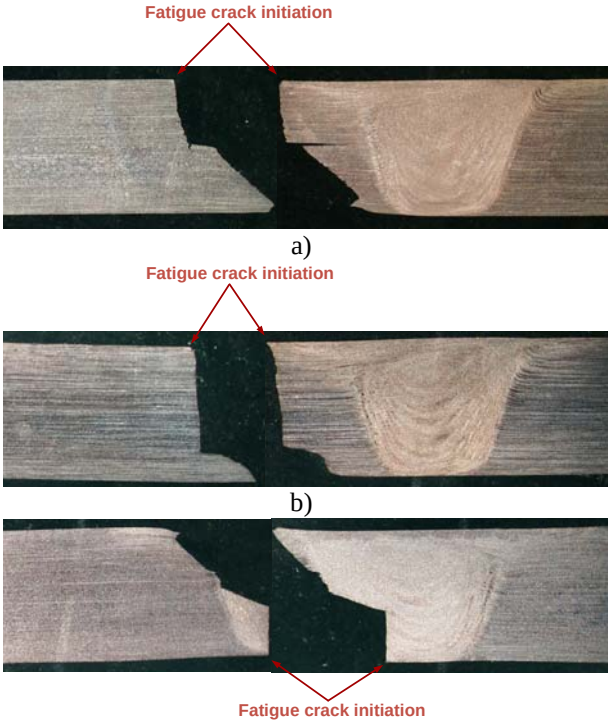

Figure 3- Fracture surface details – specimens a) IT23, b) IT26, and c) IT24.

Fracture surfaces of SN fatigue test specimens were analysed using scanning electron microscopy (SEM).
As an example of typical results found, a detail of the fracture surface at 5.93*mm* from the initiation point (spec. IT23, Fig.3a, direction perpendicular to the figure) is presented in Figure 4.

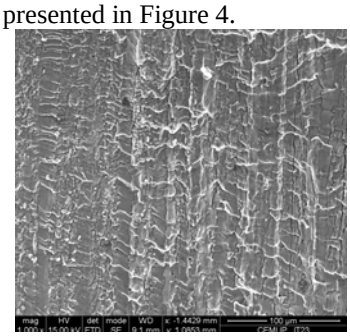

Figure 4- Detail of the fracture surface, specimen IT23.

Some details of fatigue striations in different locations along the direction mentioned are presented in **Figure 5**.

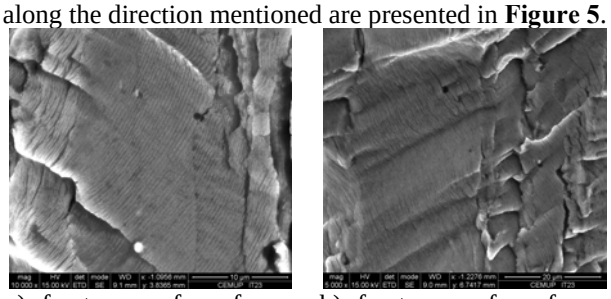

a) fracture surface for a crack length of 0.27*mm* b) fracture surface for a crack length of 3.18*mm*

Figure 5- Detail of fatigue striations, specimen IT23.

3. CRACK GROWTH

Fatigue crack growth and subsequent R-curves were evaluated according to [7, 8] considering the use of CCT specimens. The specimen geometry is presented in Figure 6 [5].

For three different R ratios, R=0.1, 0.5 and 0.8, 3 specimens were tested per each three different material conditions - base material, heat affected zone (HAZ), and weld. The R ratio 0.1 represents pressure cycling (proof test, leak test etc.), and the R ratio 0.8 the external loads during operation.
The fatigue sharpening of the spark erosion was made in order to achieve a minimum of 0.2*mm* sharp crack extension. At the end of the fatigue crack growth test K_c values and K-R curves were evaluated with a minimum remaining ligament of 15*mm*; this is described in detail in ref. [9].

A crack length of 25*mm* was obtained before loading to fracture. This crack length should be identical at INEGI and DLR to allow the comparison of K_c values between RT and cryogenic conditions. According to [5], the crack length has been chosen such that maximum possible length for crack growth evaluation and a reasonable ligament (15*mm*) before fracture can be achieved.

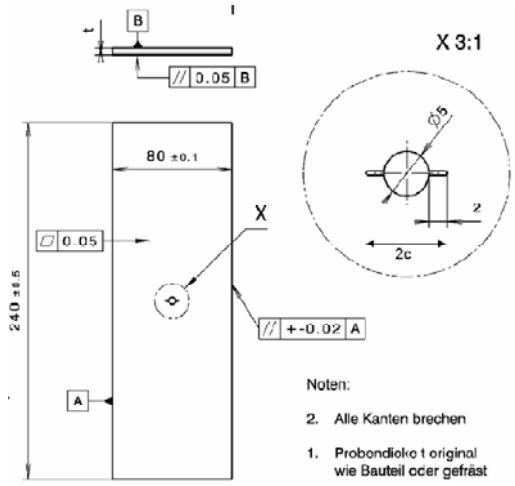

Figure 6- Definition of CCT specimen geometry.

Great experimental care was used aiming at symmetrical crack growth, which should result into a simultaneous verification of the 2a=50*mm* and (W-2a)/2=15*mm*. If unsymmetrical fatigue crack growth occurs, the criterion was to stop the fatigue crack propagation test as soon as the first ligament of 15*mm* was reached.

The specimens have notches introduced in the centre of the weld, in the HAZ and in the base material (BM), as presented in Figure 7 by lines 1, 2 and 3, respectively. The first type of specimens have notches in the centre of the weld (line 1), which coincides with the centre of the weld nugget. In the second type of specimens the crack is located in the HAZ (line 2). The positioning of the notch in the HAZ was done by MT Aerospace by slightly etching the sides of each sample, which is expected to allow a positioning of the notch according to the microstructure. The location of the notch on the retreating side is based on the position of the fracture in the integral tensile specimen at room temperature.

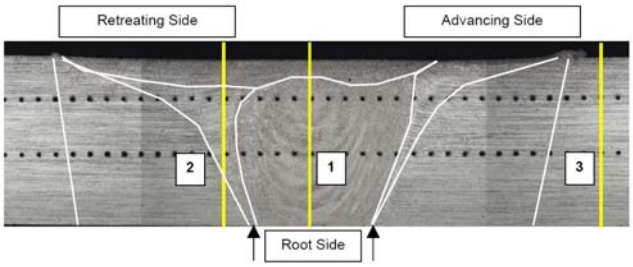

Figure 7- Through crack locations [5].

3.1 Calculation of test parameters

Table 5 presents the specimen geometry and crack size definition according to ASTM E647 [7] .

Table 5- Specimen dimension according to [7].

B [*mm*]	5
W [*mm*]	80
2a, initial crack size [*mm*]	9.4
2a, crack size before loading to fracture [*mm*]	50

According to the standard [7] for the selected type of specimen the following equation should be verified,

$$(W-2a) \geq 1.25 \cdot \frac{P_{\max}}{B \cdot \sigma_{YS}} \quad \textbf{(1)}$$

where:
$(W-2a)$ is the specimens uncracked ligament,
σ_{YS} considered to be the yield stress presented in Table 1.

Taking into consideration the material properties of the FSW material (σ_y=300MPa), when the initial crack size is considered, the maximum load should be

$$\begin{aligned} P_{\max} &\leq \frac{1}{1.25}(W-2a)B \cdot \sigma_{YS} \\ P_{\max} &\leq \frac{1}{1.25}(80-9.4)\cdot 5 \cdot 300 \\ P_{\max} &\leq 84.72kN \end{aligned} \quad \textbf{(2)}$$

For the crack size before loading to fracture the maximum load should be

$$\begin{aligned} P_{\max} &\leq \frac{1}{1.25}(80-50)\cdot 5 \cdot 300 \\ P_{\max} &\leq 36.00kN \end{aligned} \quad \textbf{(3)}$$

For defining the loads to be applied in these tests, the selection was based on considerations proposed by the project partners [5] and previous results presented by NASA [10]. So, the ΔK aimed at in these tests should start at approximately 6 $MPa.m^{0.5}$.
Taking into account this reference value and the stress intensity factor calibration proposed in the standard [7],

$$\Delta K = \frac{\left(P_{max} - R \cdot P_{max}\right)}{B} \sqrt{\frac{\pi \cdot a}{W^2}} \sec \frac{\pi \cdot a}{W} \qquad \textbf{(4)}$$

some calculations were performed in order to assess the load to be used for each R ratio.
Considering a value of ΔK=6 $MPa.m^{0.5}$, Table 6 summarises the loads that should be used for each R ratio.

Table 6- Maximum load values for each R ratio

R ratio	P_{max} [kN]
0.1	21.76
0.5	39.16
0.8	97.91

For all R ratios and considering the maximum loads presented in the previous table, the final ΔK (for the maximum crack size 2a=50mm) is 18.41 $MPa.m^{0.5}$.
Since the maximum load should be lower than 36kN, a maximum load of 35kN was considered for the specimens tested with R=0.5. If so, for this load ratio the tests will be performed for ΔK values between 5.36 and 16.45 $MPa.m^{0.5}$. These values are within the range considered of interest for this ESA TRP programme.
For R=0.8, and considering a maximum load of 35kN, ΔK values would be between 2.14 and 6.58 $MPa.m^{0.5}$. When R=0.8, according to the software ESACRACK 4 and MT Aerospace considerations, the threshold for the AA2219 T87 should be around 1.2 $MPa.m^{0.5}$. Since this material is likely to have mechanical properties approximately similar to the AA2195 T8, it is expected that both alloys present approximately similar thresholds. If so, and considering that in this project vibration loads effects are necessary for the estimation of crack growth during operation, tests will be carried out at R=0.8 with a maximum load of 35kN.
The test output of these tests includes: da/dN curve and its respective data points as well as the basic a-N data, K-R curve [8] and the load-displacement curve on which it is based, description and photography of each broken specimen, fractography and some conclusions about the crack growth in the different material zones. Because of space restrictions, only da/dN *vs* ΔK data is presented here.
The fatigue sharpening (pre-crack) was performed under constant amplitude loading and crack length was visually determined using a travelling microscope.
For the R-curve determination a displacement clip gage was used with screw attached knife edges spanning the crack at a certain span. This procedure to attach the clip gages to the specimen is in accordance to the standard ASTM E561 [8].

3.2 Test procedure and setup

Fatigue crack growth tests were carried out in a MTS 321.21 with a 250kN load cell. A mechanical grip fixture was developed in order to comply with the specimen geometry and maximum loads defined in the general test plan [5].
The crack extension was measured using a travelling microscope in each side of the specimen. In some comparisons between measurements obtained with a travelling microscope and crack gages, performed in the scope of another research project, we found that the use of a travelling microscope was the most effective system to have detailed an accurate crack length *vs.* number of cycles data.
The geometry of each specimen was accurately measured before each test, especially in the section of the material affected by the welding process.

3.3 Results

27 specimens were tested. The following paragraphs present sequentially plots of da/dN *vs.* ΔK for R=0.1, 0.5 and 0.8.

3.3.1 Specimens tested with R=0.1

Analysing the crack propagation data, Figure 8, it was verified that the higher values of crack growth rates were found for the specimens containing a notch in the centre of the weld, and the lower crack growth rates for base material specimens. The specimens with a notch in the HAZ present intermediate results. Analysing the base material specimens it is verified that for the lower ΔK values, between 6 and 8 $MPa.m^{0.5}$, there is a significant decrease of the crack growth rate. This zone corresponds to a crack growing in an irregular surface. In this figure it is also verified that for ΔK values between 10 and 11 $MPa.m^{0.5}$ data for all specimens converge to the same crack growth rate. As a future work, it should of interest to test similar specimens at ΔK values higher than 11 $MPa.m^{0.5}$.

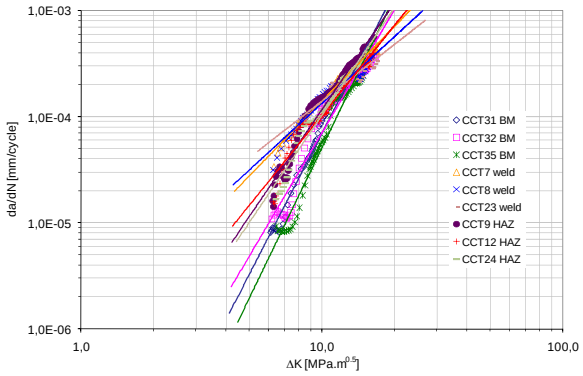

Figure 8- Crack propagation data for specimens tested with R=0.1.

3.3.2 Specimens tested with *R*=0.5

Analysing the crack propagation data, Figure 9, it was verified that for *R*=0.5 all type of specimens present similar crack growth results.

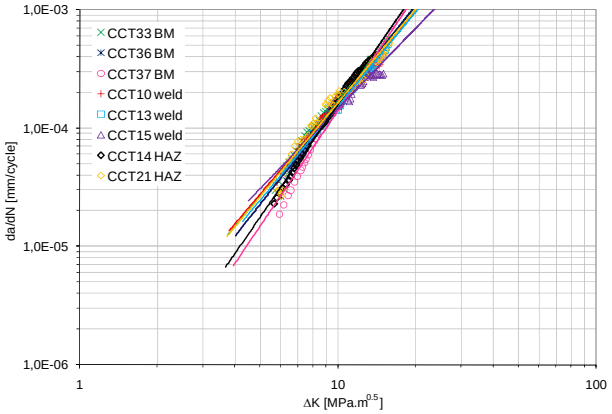

Figure 9- Crack propagation data for specimens tested with *R*=0.5.

3.3.3 Specimens tested with *R*=0.8

Analysing the crack propagation data, Figure 10, it was verified that for *R*=0.8 all type of specimens present similar crack growth results.

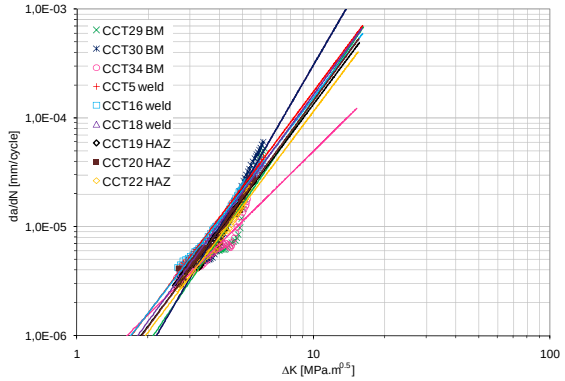

Figure 10- Crack propagation data for specimens tested with *R*=0.8.

In those cases where *ΔK* and *R* are comparable, the present *da/dN* results are in agreement of data of Hafley *et al* published by NASA, [10].

4. Concluding remarks

Good fatigue behaviour was found testing at room temperature FSW specimens of AA2195-T8X. When comparing base material and FSW SN data obtained with *R*=0.1 and 10^5 cycles the reduction of max. stress of FSW specimens is of the order of just 30%.

In those cases where *ΔK* and *R* are comparable, the present *da/dN vs ΔK* results are in agreement of existing NASA data.

Acknowledgements

The collaboration of P. Portela in the initial stages of this project, and contributions of A. Dias, D. Silva (CEMUP), F. Oliveira, J. F. R. Almeida, P. C. M. Azevedo, R. Silva, S. M. O. Tavares, V. Rêgo and J. Maeiro are acknowledged. P. Moreira acknowledges *POPH - QREN-Tipologia 4.2* – Promotion of scientific employment funded by the ESF and MCTES.

References

1. Committee on New Materials for Advanced Civil Aircraft, *New materials for next-generation commercial transports*. 1996, Washington, D.C. : National Academy Press.
2. MT Aerospace, *Cut Off Plan*, in *Damage Tolerance of Cryogenic Pressure Vessels*, E.T.R. Project, Editor. 2008.
3. ASTM E466, *Constant Amplitude Axial Fatigue Tests of Metallic Materials*.
4. ASTM E468, *Standard Practice for Presentation of Constant Amplitude Fatigue Test Results for Metallic Materials*.
5. MT Aerospace, *Fracture Mechanics Test Plan*, in *Damage Tolerance of Cryogenic Pressure Vessels*, E.T.R. Project, Editor. 2008.
6. J. P. Bonnafé, D. Gabard, and E. Grosjean, *Aluminium Lithium alloys use for reusable future launcher cryogenic metallic tanks*, in *5th Conference on Aerospace, Materials, Processes, and Environmental Technology*. 2002: Huntsville, Alabama, USA.
7. ASTM E647-05, *Standard Test Method for Measurement of Fatigue Crack Growth Rates*. 2007.
8. ASTM E561, *Standard Practice for R-Curve Determination*. 2005.
9. P.M.G.P. Moreira, P.C.M. Azevedo, M.V.A. de Figueiredo, M. Windisch, G. Sinnema, and P.M.S.T. de Castro, *Fracture and fatigue crack growth behavior of friction stir welded Al-Li 2195-T8X*, in *8º Congresso Nacional de Mecânica Experimental*. 2010: Guimarães, Portugal.
10. R. A. Hafley, J. A. Wagner, and M. S. Domack, *Fatigue Crack Growth Rate Test Results for Al-Li 2195 Parent Metal, Variable Polarity Plasma Arc Welds and Friction Stir Welds*, in *NASA/TM-2000-210098*. 2000.